

Waste metal hydroxide sludge as adsorbent for a reactive dye

Sílvia C.R. Santos, Vítor J.P. Vilar, Rui A.R. Boaventura*

LSRE-Laboratory of Separation and Reaction Engineering, Departamento de Engenharia Química, Faculdade de Engenharia da Universidade do Porto, Rua Dr. Roberto Frias, 4200-465 Porto, Portugal

Received 11 July 2007; received in revised form 9 September 2007; accepted 14 September 2007

Available online 18 September 2007

Abstract

An industrial waste sludge mainly composed by metal hydroxides was used as a low-cost adsorbent for removing a reactive textile dye (*Remazol Brilliant Blue*) in solution. Characterization of this waste material included chemical composition, pH_{ZPC} determination, particle size distribution, physical textural properties and metals mobility under different pH conditions. Dye adsorption equilibrium isotherms were determined at 25 and 35 °C and pH of 4, 7 and 10 revealing reasonable fits to Langmuir and Freundlich models. At 25 °C and pH 7, Langmuir fit indicates a maximum adsorption capacity of 91.0 mg/g. An adsorptive ion-exchange mechanism was identified from desorption studies. Batch kinetic experiments were also conducted at different initial dye concentration, temperature, adsorbent dosage and pH. A pseudo-second-order model showed good agreement with experimental data. LDF approximation model was used to estimate homogeneous solid diffusion coefficients and the effective pore diffusivities. Additionally, a simulated real effluent containing the selected dye, salts and dyeing auxiliary chemicals, was also used in equilibrium and kinetic experiments and the adsorption performance was compared with aqueous dye solutions.

© 2007 Elsevier B.V. All rights reserved.

Keywords: Waste sludge; Adsorption; Reactive dye; Equilibrium; Kinetics

1. Introduction

Dyeing operation in textile industries uses large amounts of water and generates high volumes of coloured wastewaters. A fair estimative of dye losses to the environment is about 1–2% during their production and 1–10% in their use [1]. Improper disposal of coloured wastewaters cause aesthetic problems, draws the public and authorities attention and may cause toxic effects to aquatic life.

Textile dyeing effluents are composed by complex mixtures of dyes, auxiliary chemicals, salts, acids, bases, organochlorinated compounds and occasionally heavy metals [2]. Colour removal is, however, one of the main problems in the treatment of this kind of effluents, due to dye resistance to biodegradability, light, heat and oxidizing agents [3]. Traditional treatments involving biological and coagulation/flocculation methods are generally ineffective for total colour removal. A wide range of other methods has been developed, like adsorption on organic and inorganic matrices, photocatalysis, chemical oxi-

dation, microbiological or enzymatic decomposition, etc. [4]. The removal of synthetic dyes from wastewaters is especially difficult when reactive dyes are present, for which conventional wastewater treatment plants give a low removal efficiency [5]. Dyeing with reactive dyes, mostly applied to cellulosic fibres like cotton, consists in the formation of a covalent bond between the dye and the fibre, under alkaline pH conditions and high temperatures. The hydrolysis of the dye also occurs as a secondary reaction leading to a low degree of fixation on the fibre and considerable losses of the hydrolysed dye in the effluent.

Adsorption onto solid materials has been viewed as a procedure of choice [6] on dye removal since it is an effective and economic physical method that could allow a complete decolourization of the wastewaters and their possible reuse. Activated carbon is a widely used and effective adsorbent, but the use is limited by the high costs associated with its regeneration or replacement. Literature reports several studies about the preparation of activated carbons from solid wastes and its application on dyes removal [7,8]. Low-cost materials, in their natural and modified forms, have been also extensively studied as alternative adsorbents for dyes [9–12]. In the present study, the reutilization of a waste sludge before disposal was evaluated for the adsorption of a reactive dye. This kind of waste material

* Corresponding author. Tel.: +351 225081683; fax: +351 225081674.
E-mail address: bventura@fe.up.pt (R.A.R. Boaventura).

is generated by alkalisation and consequent precipitation of the metals present in the effluents of electroplating industries and is generally composed by monomeric and polymeric metal hydroxides and salts. Few studies using waste metal hydroxide sludges as potential adsorbents have been reported in the literature. Waste Fe(III)/Cr(III) hydroxide was used for Congo Red direct dye adsorption leading to a maximum removal of 91% at pH 3 [13]. The low desorption observed indicated ion-exchange as the main process involved. Netpradit et al. [14,15] investigated reactive dyes removal by electroplating industry hydroxide sludge and obtained maximum adsorption capacities of 45.87 mg/g (for Reactive Red 120) and 61.73 mg/g (for Reactive Red 2) at 30 °C and pH 8–9. The researchers found out that the pH played an important effect on the adsorption and formation of dye–metal complexes. Another study refers to electrocoagulated metal hydroxide sludge, generated during the removal of Cr³⁺ using Al electrode, as an attractive adsorbent for Congo Red, reporting maximum adsorption capacities of 270.8 mg/g, at 30 °C and initial pH of 10.4, and 512.7 mg/g, for initial pH of 3.0 [16].

In the present work, waste metal hydroxide sludge was used for an experimental and modelling study on the adsorption equilibrium and kinetics of a reactive dye (*Remazol Brilliant Blue*). A simulated real effluent was also tested in the perspective of an industrial application of the process.

2. Materials and methods

2.1. Adsorbent preparation and characterization

A metal hydroxide sludge generated in a Portuguese zinc electroplating industry by alkaline precipitation of the metal ions present in wastewater was used as adsorbent. The sludge was firstly dried at room temperature, disaggregated, sieved in different ranges of particle sizes and dried at 105 °C overnight. The fraction 0.150–0.300 mm was selected to be further used in the experiments.

Chemical composition of the waste sludge was determined by X-ray fluorescence (XRF). Total organic carbon in the solid phase was measured according to EN 13137 and size distribution of the particles in the selected range was determined in a *Counter Coulter LS Particle Size Analyser*. Mercury porosimetry and helium picnometry were used to measure physical properties of the adsorbent.

The pH value at the zero point of charge on the surface (pH_{ZPC}) was estimated by the mass titration method proposed by Noh and Schwarz [17]. Fifty milliliter of 0.01 mol/L NaCl aqueous solutions at different initial pH values (adjusted with NaOH or HCl) were stirred with 0.150 g of waste sludge in closed Erlenmeyer flasks for 2 days at room temperature. Equilibrium pH values were then measured and pH_{ZPC} determined as the initial pH that equals final pH. Blank tests were done to take into account the possible effect of CO₂ from air.

Since sludges produced by physicochemical treatment of electroplating industries wastewaters are potentially eco-toxic residues (*EC norm 94/904*), leaching experiments were performed to evaluate the mobility of some metal species. The dried

waste sludge (1 g/L) was stirred with ultra-pure water at different pH conditions. Initial pH values were in the range 2–11 and then pH was let to natural evolution during the contact time with the waste sludge. Another experiment was done at constant pH of 4 by adjusting pH when necessary. After 24 h of contact, liquid and solid phases were separated by centrifugation, pH was measured and metal concentrations determined by atomic absorption spectrometry (*GBC 932 Plus Atomic Absorption Spectrometer*).

2.2. Adsorbate

Remazol Brilliant Blue R Special, designated hereafter as RB, was selected for this study. It is a reactive textile dye, kindly supplied by *DyStar* (Portugal), which was used in its commercial form. Table 1 presents its chemical and physical properties.

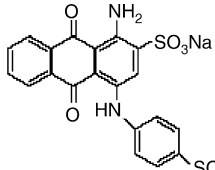
2.2.1. Aqueous dye solutions preparation

In order to obtain hydrolysed RB aqueous solutions, the desired amount of the dye was dissolved in warm distilled water. Two grams per liter of NaOH was added and solution was let to boil for 20 min. After cooling, pH was adjusted and volume was accurately made up.

2.2.2. Simulated real effluent preparation

A simulated real effluent was also prepared and used in some adsorption experiments to evaluate the effect of the presence of dyeing process auxiliaries and salts on the adsorption performance. Its preparation involved a first step where a dye bath with RB was simulated based on a standard exhaust procedure of non mercerised cotton as suggested by the dye supplier: 50 g/L of NaCl were dissolved in warm tap water and 1.0 g/L of each of the auxiliaries *Sera Wet C-AS* (anionic wetting agent), *Sera Lube M-CF* (a nonionic nature crease inhibitor and lubricant agent) and *Sera Quest M-PP* (anionic sequestrant) were added. The desired amount of RB dye (about 170 mg/L for the equilibrium study and 200 mg/L for the kinetic experiment) was then carefully dissolved at 60 °C for 20 min. Two grams per liter of NaOH and 10.0 g/L of Na₂CO₃ were added and the solution

Table 1
Physical and chemical properties of RB dye

Commercial name	Remazol Brilliant Blue R Special
Generic name	C.I. Reactive Blue 19
Chemical class	Anthraquinone
Chemical structure	
Physical state	Powder
Biodegradability	<10%
Toxicity to fishes, CL50	500–1000 mg/L (48 h, <i>Oryzias latipes</i>)
λ _{max} (nm)	593
COD (mg O ₂ /g)	1250

was maintained at constant temperature for 1 h more. Taking in account the dyeing process and the following rinse and softening baths steps industrially used, an estimated dilution of the dye bath in the final effluent by a factor of eight was considered fair. Using this hypothesis, the prepared dye bath was then accurately diluted for use in adsorption experiments.

2.2.3. Analytical method

RB dye concentrations were determined by spectrometry at the wavelength of maximum absorbance, 593 nm, in a *Helius Alpha Unicam Spectrophotometer*. A calibration curve was determined and its application was verified in the pH range of 3.5–10.5. The simulated RB effluent proved to follow the same calibration.

2.3. Adsorption equilibrium studies

2.3.1. Effect of initial pH

Batch adsorption experiments were conducted using the waste sludge as adsorbent and the RB dye in aqueous solution as adsorbate. A first set of runs were carried out to study the influence of initial and equilibrium pH on the amount of RB adsorbed. Experiments were conducted in duplicate, using an initial concentration of about 200 mg/L, an adsorbent dosage of 1.0 g/L and different values of initial solution pH between 2 and 11 (with no adjustments during the contact time). After 24 h of shaking (enough to equilibrium attainment), samples were taken out, centrifuged at 13,400 rpm (*Mini Spin Eppendorff*), equilibrium dye concentration in the liquid phase (C_{eq}) was determined by absorbance measurement and the adsorbed amount in the solid phase (q_{eq}) calculated by mass balance between the two phases. Final pH was recorded.

2.3.2. Isotherms

Adsorption equilibrium isotherms were determined at 25 °C for pH values of 4, 7 and 10, and at 35 °C at pH 7 using RB aqueous solutions. One hundred milliliter of dye solution at the required pH were magnetically stirred with different adsorbent dosages in Erlenmeyer closed flasks. pH adjustments were made when necessary to maintain a constant value, but avoiding significant changes in liquid volume. Equilibrium dye concentrations in the liquid and in the adsorbent were then determined. In order to compare the effect of the auxiliary dyeing products, the temperature and pH conditions of 25 °C and 7 were also used

to establish the equilibrium isotherm of RB dye present in the simulated effluent.

2.4. Desorption studies

In order to evaluate the mechanism involved in RB adsorption by the waste sludge, some desorption experiments were carried out under different pH conditions. The waste sludge loaded with 70.2 mg/g of RB dye was shaken with distilled water (0.20 g/50 mL) at initial pH of 2, 7, 9 and 11.5. After a contact time of 24 h, the percentage of the dye desorbed from the sludge was determined.

2.5. Adsorption kinetic studies

Adsorption dynamic experiments were performed under different conditions of temperature, initial dye concentration, waste sludge dosage and pH, according to Table 2. A volume of 0.5 L dye solution was continuously stirred at 300 rpm with the pre-established dosages of adsorbent, under constant temperature. Initial pH was adjusted with HCl or NaOH and readjusted when necessary. Samples were taken out regularly, centrifuged and the concentration evolution in the liquid phase was recorded. Equilibrium was considered to be achieved when no significant changes in dye concentration were detected.

3. Results

3.1. Characterization of the metal hydroxide sludge

Table 3 presents the chemical composition of the waste sludge obtained by XRF. The main elements are iron (26%) and zinc (21%), followed by sodium and chromium. The low organic content obtained (2.4%) indicates an essentially inorganic matrix material.

Particle size distribution (not shown) gives a mean particle size of 0.258 mm (on the basis of a volume criterion). Physical properties of the waste sludge obtained by mercury porosimetry and helium picnometry are given in Table 4. Results show the presence of mesopores and macropores and an average pore diameter of 32.3 nm. High values of porosity (>50%) were achieved. Possible agglomeration of finer particles in the waste sludge creates inter-particle spaces that could be accounted for intraparticle spaces.

Table 2
Experimental conditions used in the kinetic adsorption study

Run	Adsorbate solution	C_0 (mg/L)	m/v (g/L)	pH	T (°C)
A		200	1.0	7.0 ± 0.2	25.0 ± 0.5
B		200	1.0	7.0 ± 0.2	35.0 ± 0.5
C		36	1.0	7.0 ± 0.2	25.0 ± 0.5
D	Distilled water + dye	100	1.0	7.0 ± 0.2	25.0 ± 0.5
E		200	1.0	4.0 ± 0.3	25.0 ± 0.5
F		200	1.0	10.0 ± 0.3	25.0 ± 0.5
G		200	5.0	7.0 ± 0.2	25.0 ± 0.5
H	Simulated effluent	200	1.0	7.0 ± 0.2	25.0 ± 0.5

Table 3
Chemical composition (determined by XRF) of the waste sludge

	w/w (%)		w/w (%)
Si	1.17	Ti	0.05
Al	0.36	P	0.03
Fe	26.42	Ba	0.02
Mn	0.21	Ni	0.05
Ca	0.25	Zn	21.37
Mg	0.13	Cr	2.50
Na	4.47	Pb	0.01
K	0.28	L.I. ^a	29.06

Oxygen not included.

^a Loss on ignition.

Table 4
Textural physical properties of the waste sludge

	Hg porosimetry	He picnometry
Mean diameter (nm)	32.3	
Apparent density (g/cm ³)	1.4	
Real density (g/cm ³)		2.8
Intraparticle porosity (%)	51.3	
Total porosity (%)	52.2	51.5

Fig. 1 presents the results obtained in the determination of pH_{ZPC} of the waste sludge. pH_{ZPC} is the required pH value to give a zero net surface charge on the adsorbent. The amphoteric behaviour of the hydroxide sludge was shown by the decrease in pH due to OH^- adsorption when initial pH value was higher than 6.8 and by the increase in pH when a lower than 6.8 initial pH was used. pH_{ZPC} was then estimated as 6.8.

The liquid phase obtained in leaching experiments at different pH conditions was analyzed in terms of problematic metals and the results are shown in Table 5. In very strong acidic conditions leaching occurs in a great extent (more than 70% of the zinc and manganese and more than 60% of the iron was transferred to the liquid phase). As the initial pH increases, the trend is to decrease the concentration of the ions transferred to the aqueous solution. An experiment under constant pH of 4 was done and showed that the evolution of pH along time affects the amount of metals transferred to the solution. At constant pH 4, the zinc concentration was about 15 times greater than at initial

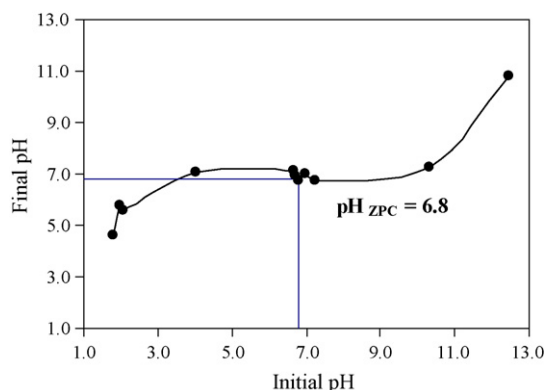


Fig. 1. Experimental determination of pH_{ZPC} .

Table 5
Leached metals concentrations obtained for different pH conditions

Initial pH	Final pH	Metals (mg/L)					
		Zn	Fe	Cr	Cu	Mn	Ni
2.0	2.2	155	158	7.46	1.04	1.55	0.15
4.0	6.8	12.3	4.59	<0.08	<0.04	0.28	<0.06
4.0 ^a	4.0	99.8	2.86	<0.08	0.38	0.67	0.15
5.0	7.0	7.30	0.66	<0.08	<0.04	<0.35	<0.06
7.0	6.8	6.61	2.34	<0.08	<0.04	<0.35	<0.06
8.0	7.2	8.10	2.70	<0.08	<0.04	<0.35	<0.06
10.0	8.3	2.53	3.71	<0.08	<0.04	<0.35	<0.06
11.0	11.3	5.82	8.74	<0.08	<0.04	<0.35	<0.06

^a pH adjustments were made to maintain a constant pH of 4.0 ± 0.3 .

pH 4. Portuguese legislation for wastewaters discharge establishes the following limits to metal concentrations: 2.0 mg/L for total chromium and nickel and 1.0 mg/L for total copper. No limit is indicated for zinc, iron or manganese. For initial pH above 2, metal concentrations in the liquid phase respect the pre-established discharge limits, but a considerable leaching of zinc occurs when pH is below 5 (Table 5). As adsorption is usually viewed as a tertiary treatment, pH of the previously treated effluents is generally neutral and, in these conditions, leaching from the sludge is insignificant and a safe discharge is achieved when using this adsorbent.

3.2. Adsorption equilibrium studies

3.2.1. Effect of initial pH

The effect of initial and equilibrium pH on the amount of dye adsorbed using constant initial dye concentration and adsorbent dosage is shown in Fig. 2. It can be seen that the increase in initial pH values leads to a decrease in the adsorption extent, which is more visible in the ranges 2–5 and 9–11. Between 5.0 and 9.0, the effect of initial pH is not much significant when the pH evolution is very close to pH values at equilibrium. Maximum adsorbed amount (176 mg/g) was achieved at pH 2 and minimum adsorbed amount (20.3 mg/g) was obtained at pH 11. This kind of behaviour, extensively reported in literature, is the result of the effect of pH on the surface charge of the adsorbent, where

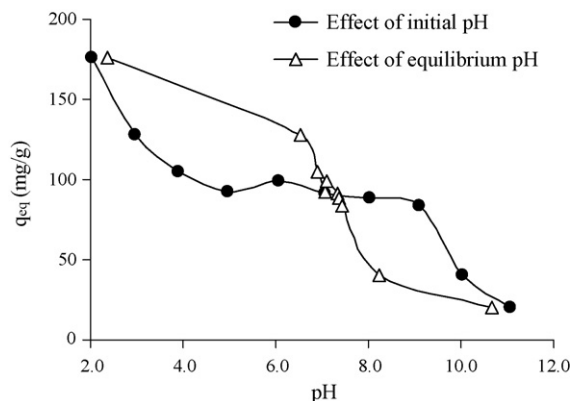


Fig. 2. Effect of the initial and equilibrium solution pH on the amount of RB dye adsorbed (initial dye concentration ≈ 200 mg/L, $T = 25^\circ\text{C}$).

acidic conditions develop a positive charge resulting in higher adsorption of anionic species. Below pH_{ZPC} (6.8), favourable positive charge conditions occur for the adsorption of negatively charged species. An identical behaviour was reported for the removal of Congo Red by electrocoagulated metals hydroxide sludge, which showed a marked increase of the removal as the pH decreased [16]. A different behaviour, where a maximum removal was achieved at pH 8–9, near pH_{ZPC} , was also reported [14].

3.2.2. Equilibrium isotherms

Adsorption isotherms of RB dye onto the waste sludge are illustrated in Fig. 3. The experimental data were fitted to Langmuir and Freundlich models. Langmuir isotherm [18] is expressed by:

$$q_{eq} = \frac{Q_{max} K_L C_{eq}}{1 + K_L C_{eq}} \quad (1)$$

where Q_{max} is the maximum adsorption capacity, corresponding to a monolayer coverage and K_L is the Langmuir constant related to the energy of adsorption. Freundlich isotherm [19] is represented by:

$$q_{eq} = K_F C_{eq}^{1/n} \quad (2)$$

where K_F and $1/n$ are the model parameters related to the adsorption capacity and adsorption intensity, respectively. Experimental results were fitted to Eqs. (1) and (2) by nonlinear regression, using the software *Fig.P* from *Biosoft*. The obtained values of the parameters and the statistical data are given in Table 6. The determination coefficients (R^2) suggest that a better fit was obtained using the Langmuir model. However, the F -test is a more suitable tool to compare the applicability of both models. The values of F , calculated as the ratio between the variances of the two models, are always below the tabulated F -value for 95% confidence level, indicating that both models can be used to describe the experimental data because they are not statistically different. Fig. 3a shows the effect of temperature on the amount of dye adsorbed at pH 7. We can observe that temperature does not significantly affect the extent of adsorption in the range usually found in effluents from textile dyeing industries (25–35 °C). Fig. 3b shows the effect of pH on the adsorption capacity for $T=25$ °C. The maximum adsorption capacity given by the Langmuir fitting is 275 mg/g at pH 4, about three times greater than the capacity obtained at neutral conditions (91.0 mg/g). At constant pH 10, the uptake capacity is much lower. It is also evident from

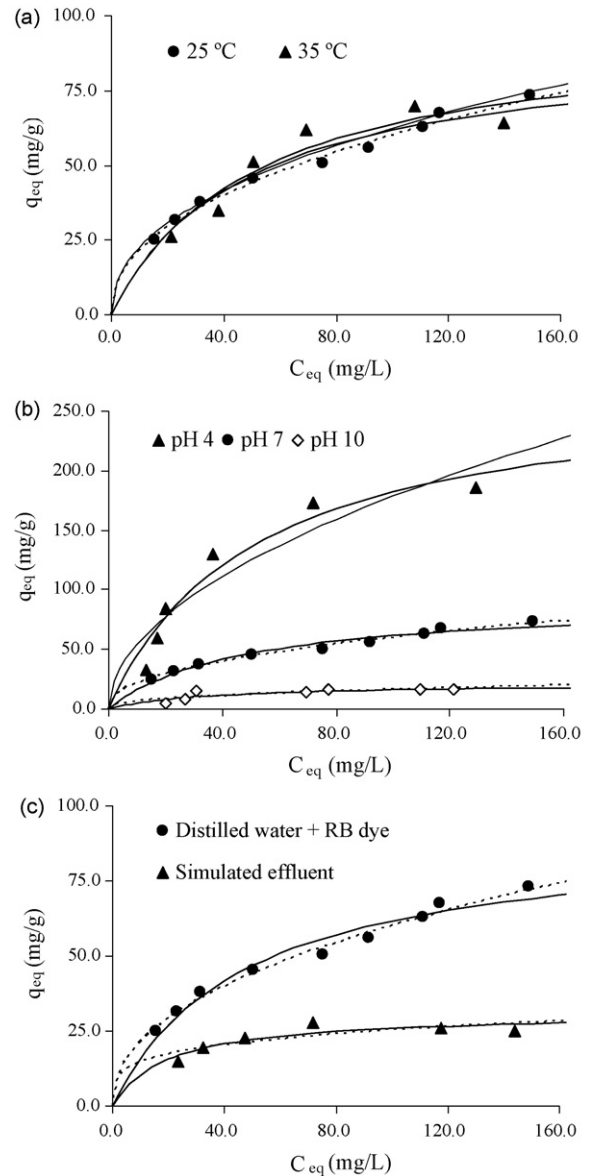


Fig. 3. Equilibrium adsorption isotherms. (a) RB in aqueous solution, pH 7, $T=25$ and 35 °C; (b) RB in aqueous solution, 25 °C, different pH values; (c) RB in aqueous solution and simulated effluent, 25 °C, pH 7; Langmuir (—) and Freundlich (---) models.

Fig. 3b the decrease of the dye affinity to the surface (given by the slope of the isotherm curve at low dye concentration) when pH increases. The comparison between the use of a simple dye aqueous solution and a simulated textile effluent is illustrated in

Table 6
Equilibrium isotherms modelling: parameters (\pm standard error) and statistical data

T (°C)	pH	Langmuir			Freundlich			F_{calc}	$F_{\alpha=0.05}$
		Q_{max} (mg/g)	$K_L \times 10^2$ (L/mg)	R^2	K_F (mg/g/(mg/L) $^{1/n}$)	n	R^2		
25	7	91 ± 6	2.10 ± 0.38	0.96	7.6 ± 0.9	2.2 ± 0.1	0.98	2.2	3.4
35	7	97 ± 15	1.94 ± 0.74	0.90	8.1 ± 4.0	2.3 ± 0.6	0.83	1.7	5.1
25	4	275 ± 45	1.95 ± 0.68	0.94	16.5 ± 7.9	1.9 ± 0.4	0.87	2.0	5.1
25	10	22 ± 5	2.81 ± 1.70	0.72	2.5 ± 1.6	2.5 ± 0.9	0.66	1.2	4.3
25	7 ^a	31 ± 3	5.06 ± 1.92	0.81	8.5 ± 3.2	4.2 ± 1.6	0.67	1.7	5.1

^a Simulated effluent.

Fig. 3c. At 25 °C and pH 7, the isotherm of the simulated effluent indicates a marked decrease in the affinity of the dye by the adsorbent and in the amount of dye adsorbed, corresponding to a 66% reduction of the maximum adsorption capacity. The presence of salts, like Na₂CO₃ and NaCl, and auxiliary dyeing chemicals, affects negatively the adsorption. The coverage of the adsorbent surface, the possible blockage of pores and the possibility of existing competition (among dye and wetting anionic species and the sequestrant agents, for example) could explain this observation.

Few materials have been tested and reported in literature as adsorbents for Reactive Blue 19 dye. Iqbal and Saeed [20] evaluated fungal biomass (*Phanerochaete chrysosporium*) in free and in loofa sponge immobilized states and obtained Langmuir maximum adsorption capacities of 80.91 and 98.80 mg/g, respectively, at pH 2.0 and 30 °C. In other study, using wheat bran as adsorbent, uptake capacities of 97.1 mg/g (20 °C) and 117.7 mg/g (60 °C) were obtained at pH 1.5 [21]. A DTMA bromide—modified bentonite revealed also good adsorption capacities, 3.30×10^{-4} mol/g (about 207 mg/g), at pH 1.5 and temperature of 20 °C [22]. In the present study, the maximum adsorption capacity at pH 4 (275 mg/g) is greater than those values reported in literature. It is important to point out that the strong acidic pH conditions are the most favourable to the adsorption extent but have a limited interest from a practical point of view, as textile dyeing effluents are usually alkaline.

3.3. Desorption studies

Fig. 4 shows the results obtained in desorption experiments using RB-loaded waste sludge. It was found that under acidic and neutral pH, low desorption occurred (3–10%) suggesting no predominance of weak physical bonds. Using strong alkaline conditions more than 50% of the adsorbed dye was further desorbed confirming the ion-exchange as the main process related with RB adsorption [23]. Since about of 44% of the dye still remained in the solid phase even at pH of 11.5, strong chemical bonds could be probably also involved in adsorption. Ion exchange has been reported as the main mechanism involved in the adsorption of reactive and direct dyes onto this kind of material [14,16].

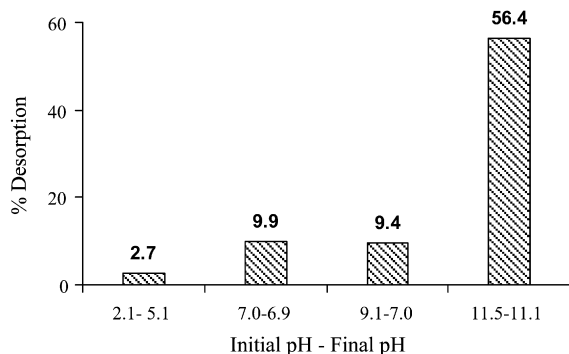


Fig. 4. RB desorption from saturated waste sludge under different pH conditions.

3.4. Kinetic studies

3.4.1. Modelling

Several models have been used to describe adsorption kinetics, but pseudo-first and pseudo-second-order models are the most common. Pseudo-first-order rate model or Lagergren and Svenska model [24] is given by:

$$\frac{dq}{dt} = k_1(q_{eq} - q) \quad (3)$$

where q and q_{eq} are the concentrations of the adsorbate on the solid phase per adsorbent mass unity at time t and at equilibrium, respectively, and k_1 is the rate constant. Integrating Eq. (3) with the boundary conditions $t=0, q=0$ and $t=t, q=q$, the following expression is obtained:

$$q = q_{eq}[1 - \exp(-k_1t)] \quad (4)$$

The pseudo-second-order rate model is expressed by [25]:

$$\frac{dq}{dt} = k_2(q_{eq} - q)^2 \quad (5)$$

where k_2 is the rate constant. The integration of Eq. (5) with the same boundary conditions ($t=0, q=0$; $t=t, q=q$), gives:

$$q = q_{eq} \frac{k_2 q_{eq} t}{1 + k_2 q_{eq} t} \quad (6)$$

Although the pseudo-first and pseudo-second-order models generally describe the adsorption process, these models are useless for the determination of the adsorption mechanism. Adsorption kinetics depends on a multi-step process involving the transport of the adsorbate from the bulk solution, diffusion in the external film to the surface of the adsorbent, intraparticle diffusion in the pores and in the solid phase and finally adsorption on the sites. In well stirred batch systems, it is likely that the intraparticle diffusion is the rate controlling step. Linear driving force (LDF) approximation [26] assumes that the uptake of the adsorbate is linearly proportional to a driving force defined as the difference between the adsorbed amount at the surface (q_s) and the average adsorbed amount in the adsorbent (q):

$$\frac{\partial q}{\partial t} = k_{LDF}(q_s - q) \quad (7)$$

The overall mass balance for batch adsorption experiments is given by:

$$q = (C_0 - C) \frac{v}{m} \quad (8)$$

where C_0 and C are the dye concentrations in the liquid phase at the $t=0$ and at time t , respectively, and m/v is the adsorbent dosage.

The adsorbed amount at the surface of the adsorbent is in equilibrium with the bulk concentration is assumed to be given by Langmuir isotherm:

$$q_s = \frac{Q_{max} K_L C}{1 + K_L C} \quad (9)$$

Substituting Eqs. (8) and (9) in Eq. (7) and introducing the dimensionless variables

$$\xi = \frac{Q_{\max} m}{C_0 v}; \quad y = \frac{C}{C_0} \quad (10)$$

an ordinary differential is obtained:

$$\frac{dy}{dt} + k_{LDF} \left(\frac{\xi K_L C_0}{1 + K_L C_0 y} + 1 \right) y = k_{LDF} a_p \quad (11)$$

Eq. (11) has an analytical solution for the limit conditions $t=0$, $y=1$ and $t=t$, $y=y$, in the form of time (t) versus dimensionless concentration (y), given by [27]:

$$t = \frac{1}{k_{LDF}} \left\{ \frac{1}{2b} \ln \left[\frac{y^2 + ay - b}{a - b + 1} \right] + \left(1 - \frac{a}{2b} \right) \left(\frac{1}{\alpha - \beta} \right) \ln \right. \\ \left. \times \left[\frac{(1 - \beta)(y - \alpha)}{(1 - \alpha)(y - \beta)} \right] \right\} \quad (12)$$

where

$$a = \xi - 1 + \frac{1}{K_L C_0}; \quad b = \frac{1}{K_L C_0}; \\ \alpha = \frac{-a + \sqrt{a^2 + 4b}}{2}; \quad \beta = \frac{-a - \sqrt{a^2 + 4b}}{2} \quad (13)$$

Homogeneous solid diffusion model (HSDM) was developed for homogeneous particles, but has been applied to porous particles in several adsorption systems [27–29]. Supposing a parabolic profile of dye concentration as a function of radial position inside the particle, the following expression is obtained from HSDM model:

$$\frac{\partial q}{\partial t} = \frac{15 D_h}{R^2} (q_s - q) \quad (14)$$

Conjugating Eq. (14) with Eq. (7), we get:

$$k_{LDF} = \frac{15 D_h}{R^2} \quad (15)$$

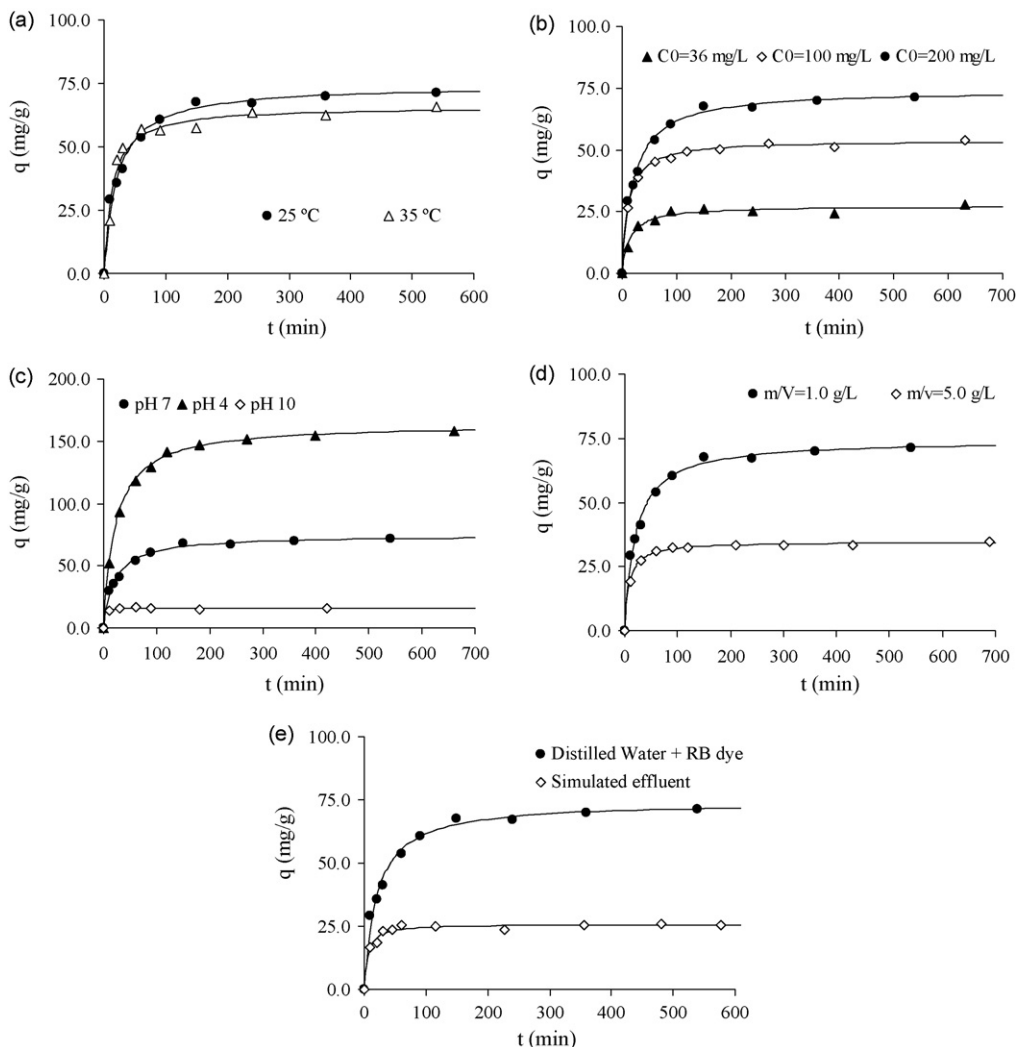


Fig. 5. Experimental data and pseudo-second-order modelling of RB adsorption kinetics. Effect of (a) temperature (runs A and B); (b) initial dye concentration (runs A, C and D); (c) pH (runs A, E and F); (d) adsorbent dosage (runs A and G) and (e) chemicals in the simulated effluent (runs A and H).

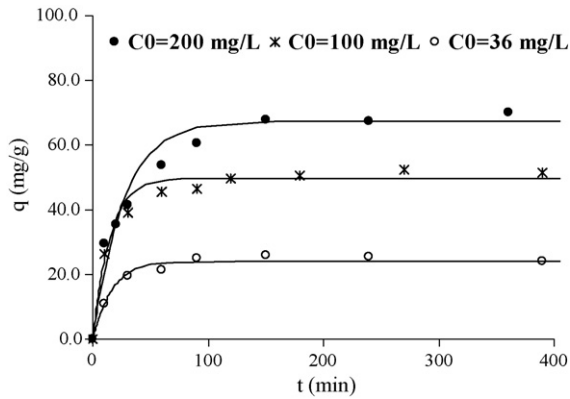


Fig. 6. LDF approximation modelling of RB adsorption kinetics.

Eq. (15) allows estimating the homogeneous diffusion coefficient, D_h .

Considering the diffusion into the pores of the adsorbent, the effective pore diffusivity (D_{Pe}) can be calculated from [30]:

$$k_{LDF} = \frac{\Omega D_{Pe}}{\rho_s R^2 \Delta q / \Delta C} \quad (16)$$

where Ω is a constant related to the geometric shape of particles (15 for spherical particles) and $\Delta q / \Delta C$ is the mean slope of the equilibrium isotherm.

Kinetic results are presented in Figs. 5 and 6. The removal of RB is fast in the first hour (more than 72% of the maximum adsorbed amount was attained for all experiments) and then a slow gradual removal of the dye still occurs up to adsorbent saturation in about 10 h. For the experiments conducted at pH 10 and the experiment carried out with the simulated effluent, no significant changes in the liquid phase dye concentration were detected after the first hour and so equilibrium was assumed to be achieved.

The experimental data were fitted to the pseudo-first and pseudo-second-order models, Eqs. (4) and (6), and the obtained parameters are given in Table 7. Taking into account the R^2 values, both models provided good adjustment to the kinetic data. F -test indicates no statistical difference between the performance of the two models for experiments B, C, F and H but a clearly better performance of pseudo-second-order model in the case of runs A, D, E and G. Therefore, the pseudo-second-order model seems to describe more appropriately the RB adsorption

Table 8

LDF approximation fit parameter and homogeneous solid and effective pore diffusion coefficients

Run	LDF		D_h (cm ² /s)	D_{Pe} (cm ² /s)
	k_{LDF} (min ⁻¹)	R^2		
A	0.145	0.97	2.68×10^{-8}	7.27×10^{-6}
B	0.157	0.93	2.89×10^{-8}	3.97×10^{-6}
C	0.024	0.97	4.42×10^{-9}	1.12×10^{-5}
D	0.095	0.92	2.22×10^{-8}	3.21×10^{-5}
G	0.140	0.95	2.59×10^{-8}	1.54×10^{-5}

kinetics. Fig. 5 shows the predicted pseudo-second-order curves for all the kinetic experiments.

LDF approximation model, Eq. (12), was also fitted to the experimental data for different initial dye concentrations, temperature and adsorbent dosages (runs A–D and G), by minimizing the sum of residuals between experimental and predicted curves. Fig. 6 shows, as an illustrative example, the LDF predicted curves for different initial dye concentrations. Eqs. (15) and (16) were further used to calculate the homogeneous diffusion coefficient and the effective pore diffusivity (Table 8).

3.4.2. Temperature effect

Fig. 5a shows the effect of temperature on the dynamic adsorption data of RB by the waste sludge. Temperature is known to have an enhancement effect on adsorption dynamics due to the increased rate of diffusion across the external (here neglected) and internal pores of the adsorbent. Diffusivity values (Table 8) indicate a slightly higher D_h but a lower D_{Pe} for 35 °C than for 25 °C.

3.4.3. Initial dye concentration effect

Initial dye concentration influence on adsorption dynamics is shown in Fig. 5b. Raising the initial RB concentration from 36 to 200 mg/L the adsorbent capacity increased from 27.3 to 74.3 mg/g. The pseudo-second-order rate constant, k_2 , decreased almost linearly with the initial concentration increase, showing that the process is highly concentration dependent. The homogeneous diffusion coefficient increased with the initial dye concentration due to the increase in surface coverage. A similar trend was reported in adsorption of basic dyes by granular activated carbon and zeolite [31], where a linear effect was observed. Effective pore diffusivity however does not show

Table 7

Adsorption kinetic modelling: parameters (\pm standard error) and statistical data

Run	Pseudo-first order			Pseudo-second order			F_{calc}	$F_{\alpha=0.05}$	
	$k_1 \times 10^2$ (min ⁻¹)	q_{eq} (mg/g)	R^2	$k_2 \times 10^3$ (g/mg/min)	q_{eq} (mg/g)	R^2			$r_{initial}$ (mg/g/min)
A	3.3 ± 0.4	68.9 ± 2.1	0.97	0.65 ± 0.06	74.3 ± 1.2	0.99	3.61	4.4	3.0
B	5.3 ± 0.6	61.5 ± 1.4	0.97	1.2 ± 0.2	65.8 ± 1.9	0.97	5.15	1.2	3.0
C	4.6 ± 0.6	25.7 ± 0.6	0.98	2.6 ± 0.4	27.3 ± 0.6	0.99	1.97	1.7	3.2
D	5.8 ± 0.8	50.7 ± 1.1	0.97	1.7 ± 0.1	53.9 ± 0.4	1.0	4.82	11.0	3.0
E	2.9 ± 0.3	152 ± 3	0.98	0.28 ± 0.01	164 ± 1	1.0	7.42	23.0	3.0
F	22.8 ± 4.0	15.9 ± 0.3	0.99	54 ± 29	16.1 ± 0.4	1.0	14.08	1.2	4.3
G	7.5 ± 0.8	33.1 ± 0.5	0.98	3.7 ± 0.2	34.7 ± 0.2	1.0	4.39	16.2	3.0
H	9.1 ± 1.0	24.8 ± 0.5	0.98	7.1 ± 0.1	25.9 ± 0.5	0.98	4.74	1.2	3.0

a consistent behaviour with the initial concentration since it increased in the concentration range 36–100 mg/L but decreased in the range 100–200 mg/L. This phenomenon may be due to collisions between dye molecules or agglomeration at high concentrations in the bulk solution and increase in the resistance within particles [32].

3.4.4. Adsorbent dosage effect

Fig. 5c compares dynamic adsorption curves at different adsorbent dosages for constant initial dye concentration, pH and temperature. Using a dosage of 5.0 g/L the amount of dye adsorbed at equilibrium per gram of adsorbent is about half the amount adsorbed using 1.0 g/L, as could be seen in experimental and predicted results. The decrease in adsorbed amount at equilibrium when increasing the waste sludge dosage is due to the unsaturated adsorption sites that remain during the adsorption process [33]. Homogeneous diffusivity values obtained for the two adsorbent dosages are almost similar; a slightly lower value was obtained for the higher dosage. Decreasing adsorbent mass, the slope of the operation line increases while the slope of the adsorption isotherm at the final equilibrium concentration decreases and the surface coverage increases [28].

3.4.5. pH effect

Studies on the effect of pH (Fig. 5d) indicate a low adsorbed amount at pH 10, almost (90%) attained in the first 10 min. The initial adsorption rates (r_{initial}), calculated from the pseudo-second-order equation, are 7.42, 3.61 and 14.1 mg g⁻¹ min⁻¹, respectively, for pH 4, 7 and 10.

3.4.6. Simulated effluent

The effect of using a simulated RB effluent is illustrated in Fig. 5e. The initial adsorption rate is greater when using the simulated effluent (Table 7) and after 1 h contact time the adsorbent is already saturated. Nevertheless, for the RB solution prepared with distilled water, the maximum uptake capacity is about three times higher, which is in accordance with the equilibrium results.

4. Conclusions

The influence of temperature, pH and the presence of dyeing auxiliary chemicals and salts on the removal *Remazol Blue* reactive dye in aqueous solution by a waste metal hydroxide sludge was evaluated.

Equilibrium data were well described by both Langmuir and Freundlich models. The maximum adsorption capacities obtained varied between 275 mg/g (at 25 °C and pH 4) and 21.9 mg/g (at 25 °C and pH 10). When a simulated textile effluent was used as adsorbate, a decrease in the adsorption capacity from 91.0 to 31.0 mg/g was observed. Desorption studies suggested that strong chemical bonds, namely ion-exchange, are involved in the adsorption process.

Kinetic data were adequately fitted by the pseudo-second-order kinetic model. Homogeneous and pore effective diffusivities of the reactive dye in the adsorbent particles were estimated by fitting kinetic data to LDF approximation model and homogeneous solid diffusion model (HSDM).

The waste metal hydroxide sludge showed to be an interesting adsorbent for *Remazol Blue* but its performance is worse when treating textile dyeing effluents. The metal constituents of the sludge are not leached for pH > 4.

Acknowledgement

The authors are grateful to Portuguese Foundation for Science and Technology (FCT) for S. Santos' scholarship (SFRH/BD/18477/2004).

References

- [1] E. Forgacs, T. Cserhati, G. Oros, Removal of synthetic dyes from wastewaters: a review, *Env. Int.* 30 (7) (2004) 953–971.
- [2] I.M. Gonçalves, M.I. Ferra, M.T.P. Amorim, Processos de remoção biológica de corantes nos efluentes de indústria têxtil, *Tecnologias do Ambiente* 11 (1996) 35–38.
- [3] Q.Y. Sun, L.Z. Yang, The adsorption of basic dyes from aqueous solution on modified peat-resin particle, *Water Res.* 37 (7) (2003) 1535–1544.
- [4] O.J. Hao, H. Kim, P.C. Chiang, Decolorization of wastewater, *Crit. Rev. Env. Sci. Technol.* 30 (4) (2000) 449–505.
- [5] K. Kumari, T.E. Abraham, Biosorption of anionic textile dyes by nonviable biomass of fungi and yeast, *Bioresour. Technol.* 98 (9) (2007) 1704–1710.
- [6] G. Crini, Non-conventional low-cost adsorbents for dye removal: a review, *Bioresour. Technol.* 97 (9) (2006) 1061–1085.
- [7] K. Kadirvelu, M. Kavipriya, C. Karthika, M. Radhika, N. Vennilamani, S. Pattabhi, Utilization of various agricultural wastes for activated carbon preparation and application for the removal of dyes and metal ions from aqueous solutions, *Bioresour. Technol.* 87 (1) (2003) 129–132.
- [8] Y. Onal, Kinetics of adsorption of dyes from aqueous solution using activated carbon prepared from waste apricot, *J. Hazard. Mater.* 137 (3) (2006) 1719–1728.
- [9] A.A. Ahmad, B.H. Hameed, N. Aziz, Adsorption of direct dye on palm ash: kinetic and equilibrium modeling, *J. Hazard. Mater.* 141 (1) (2007) 70–76.
- [10] A. Gurses, C. Dogar, M. YalcIn, M. AelkyIldiz, R. Bayrak, S. Karaca, The adsorption kinetics of the cationic dye, methylene blue, onto clay, *J. Hazard. Mater.* 131 (1–3) (2006) 217–228.
- [11] Z. Aksu, S. Tezer, Equilibrium and kinetic modelling of biosorption of *Remazol Black B* by *Rhizopus arrhizus* in a batch system: effect of temperature, *Proc. Biochem.* 36 (5) (2000) 431–439.
- [12] B. Acemioglu, Adsorption of Congo Red from aqueous solution onto calcium-rich fly ash, *J. Colloid Interface Sci.* 274 (2) (2004) 371–379.
- [13] C. Namasivayam, R. Jeyakumar, R.T. Yamuna, Dye removal from wastewater by adsorption on waste Fe(III)/Cr(III) hydroxide, *Waste Manage.* 14 (7) (1994) 643–648.
- [14] S. Netpradit, P. Thiravetyan, S. Towprayoon, Application of 'waste' metal hydroxide sludge for adsorption of azo reactive dyes, *Water Res.* 37 (4) (2003) 763–772.
- [15] S. Netpradit, P. Thiravetyan, S. Towprayoon, Adsorption of three azo reactive dyes by metal hydroxide sludge: effect of temperature, pH, and electrolytes, *J. Colloid Interface Sci.* 270 (2) (2004) 255–261.
- [16] A.K. Golder, A.N. Samanta, S. Ray, Anionic reactive dye removal from aqueous solution using a new adsorbent—sludge generated in removal of heavy metal by electrocoagulation, *Chem. Eng. J.* 122 (1–2) (2006) 107–115.
- [17] J.S. Noh, J.A. Schwarz, Estimation of the point of zero charge of simple oxides by mass titration, *J. Colloid Interface Sci.* 130 (1) (1989) 157–164.
- [18] I. Langmuir, The adsorption of gases on plane surfaces of glass, mica and platinum, *J. Am. Chem. Soc.* 40 (1918) 1361–1403.
- [19] H.M.F. Freundlich, Over the adsorption in solution, *J. Phys. Chem.* 57 (1906) 385–471.

- [20] M. Iqbal, A. Saeed, Biosorption of reactive dye by loofa sponge-immobilized fungal biomass of *Phanerochaete chrysosporium*, Proc. Biochem. 42 (7) (2007) 1160–1164.
- [21] F. Cicek, D. Ozer, A. Ozer, A. Ozer, Low cost removal of reactive dyes using wheat bran, J. Hazard. Mater. 146 (1–2) (2007) 408–416.
- [22] A. Ozcan, C. Omeroglu, Y. Erdogan, A.S. Ozcan, Modification of bentonite with a cationic surfactant: an adsorption study of textile dye Reactive Blue 19, J. Hazard. Mater. 140 (1–2) (2007) 173–179.
- [23] G. McKay, G. Ramprasad, P. Mowli, Desorption and regeneration of dye colors from low-cost materials, Water Res. 21 (3) (1987) 375–377.
- [24] S. Langergren, B.K. Svenska, Zur theory der sogenannten adsorption geloster stoffe, Veternskapsakad Handlingar 24 (4) (1898) 1–39.
- [25] Y.S. Ho, G. McKay, Pseudo-second-order model for sorption processes, Proc. Biochem. 34 (5) (1999) 451–465.
- [26] E. Glueckauf, Theory of chromatography. Part 10. Formulae for diffusion into spheres and their application to chromatography, Tans. Faraday Soc. 51 (1955) 1540–1554.
- [27] V.J.P. Vilar, C.M.S. Botelho, R.A.R. Boaventura, Equilibrium and kinetic modelling of Cd(II) biosorption by algae *Gelidium* and agar extraction algal waste, Water Res. 40 (2) (2006) 291–302.
- [28] V. Meshko, L. Markovska, M. Mincheva, Two resistance mass transfer model for the adsorption of basic dyes from aqueous solution on natural zeolite, Bull. Chem. Technol. Macedonia 18 (2) (1999) 161–169.
- [29] G. McKay, Application of surface diffusion model to the adsorption of dyes on bagasse pith, Adsorption 4 (3–4) (1998) 361–372.
- [30] E. Glueckauf, J.I. Coates, Theory of chromatography. 4. The influence of incomplete equilibrium on the front boundary of chromatograms and on the effectiveness of separation, J. Chem. Soc. (1947) 1315–1321.
- [31] V. Meshko, L. Markovska, M. Mincheva, A.E. Rodrigues, Adsorption of basic dyes on granular activated carbon and natural zeolite, Water Res. 35 (14) (2001) 3357–3366.
- [32] G.M. Walker, L.R. Weatherley, Kinetics of acid dye adsorption on GAC, Water Res. 33 (8) (1999) 1895–1899.
- [33] Y. Bulut, H. Aydin, A kinetics and thermodynamics study of methylene blue adsorption on wheat shells, Desalination 194 (1–3) (2006) 259–267.